

On the Saturation of Astrophysical Dynamos: Numerical Experiments with the No-cosines flow

S.B.F. Dorch

The Niels Bohr Institute for Astronomy, Physics and Geophysics, Juliane Maries Vej 30, DK-2100 Copenhagen Ø, Denmark

V. Archontis

Instituto de Astrofísica de Canarias, Via Lactea s/n E-38200, La Laguna, Spain

August 16, 2004

Abstract. In the context of astrophysical dynamos we illustrate that the no-cosines flow, with zero mean helicity, can drive fast dynamo action and study the dynamo's mode of operation during both the linear and non-linear saturation regime: It turns out that in addition to a high growth rate in the linear regime, the dynamo saturates at a level significantly higher than normal turbulent dynamos, namely at exact equipartition when the magnetic Prandtl number $\text{Pr}_m \sim 1$. Visualization of the magnetic and velocity fields at saturation will help us to understand some of the aspects of the non-linear dynamo problem.

Keywords: Magnetic fields, MHD, turbulence, diffusion, Sun, stars

1. Introduction

Magnetic fields are common in astronomical objects and are responsible for a variety of complex phenomena in the Universe: It is widely accepted that these fields are generated by the motions of conducting fluids through a transfer of kinetic to magnetic energy, that is, dynamo action (Parker, 1979). However, our understanding of the exact mechanism of generation and maintenance of the magnetic field against dissipation is still incomplete even for simple dynamos. On the observational side, when a magnetic field in an astronomical object is not observed directly often the inferred equipartition value $B_{\text{eq}} = u\sqrt{\mu_0\rho}$ (where u and ρ are characteristic speed and mass density, and μ_0 is the vacuum permeability) is assumed, e.g. Safier (1999): Therefore it is of importance to consider whether this is a good approach. In the Sun the equipartition field strength at the surface is about 500 Gauss. However, the mean magnetic field strength near the Sun's polar regions has a canonical value of 1–5 G going back to Babcock, which is far less than B_{eq} ; additionally, the intermittent flux tubes at the surface is much stronger, with field strengths around 1–3 kG in spots and flux tubes, while it is inferred to be 10 kG near the bottom of the convection zone, e.g. Moreno-Insertis et al. (1994). In any case B_{eq} is not a good



© 2018 Kluwer Academic Publishers. Printed in the Netherlands.

estimate for the solar magnetic field. Furthermore, on the theoretical side of things, numerical models of turbulent non-linear dynamo action as a rule produce strong intermittent structures, but cannot be said to generally saturate at equipartition; these models can be used to study the generic properties of real astrophysical dynamos, such as the solar dynamo (Choudhuri, 2003).

Dynamo action in the limit of infinite magnetic Reynolds number $\text{Re}_m = u\ell/\eta$ (where ℓ is a characteristic length scale and η is the magnetic diffusivity) is relevant to astrophysical systems where the diffusion time-scale is larger than the advection time-scale, such as in the Sun. Considering the importance of the magnetic forces relative to the motion of the fluid, one divides dynamo action into two regimes: The linear kinematic regime in which the flow amplifies the magnetic field exponentially by e.g. stretching the magnetic field lines (Childress & Gilbert, 1995) and the non-linear regime where the magnetic field becomes strong enough to modify the initial flow topology through the Lorentz force and saturate the exponential growth.

Recent studies (Dorch, 2000; Archontis et al., 2003a; Tanner & Hughes, 2003) have improved our knowledge of fundamental dynamo mechanisms of prescribed flows in the kinematic regime. Non-linear fast dynamo action has received considerable attention and progress has been made especially by means of numerical magneto-hydrodynamical (MHD) simulations (Nordlund et al., 1992; Cattaneo et al., 1996). However, it is still unclear what are the physical processes at work before and especially after the saturation of the dynamo: It is generally found that dynamos saturate because of a suppression of the stretching ability of the flows (Cattaneo et al., 1996; Archontis et al., 2003b; Tanner & Hughes, 2003), but the details of how this comes about are not known.

In this paper, we present results from numerical experiments with a non-helical flow first studied by Galloway & Proctor (1992) that saturates below equipartition only for high values of the Reynolds number $\text{Re} = u\ell/\nu$ (ν being the viscosity): At magnetic Prandtl number $\text{Pr}_m = \text{Re}_m/\text{Re} \sim 1$ saturation occurs at almost exact equipartition. We study the non-linear dynamo mode of operation, examine how it changes when the flow becomes turbulent, and take the first steps at illustrating how the fields evolve and interact.

2. Setup of the numerical experiments

The fully compressible 3-d MHD equations are solved numerically on a periodic Cartesian grid:

$$\frac{\partial \rho}{\partial t} = -\nabla \cdot \rho \mathbf{u}, \quad (1)$$

$$\frac{\partial(\rho \mathbf{u})}{\partial t} = -\nabla P + \mathbf{j} \times \mathbf{B} + \mathbf{f} - \nabla \cdot (\rho \mathbf{u} \mathbf{u}), \quad (2)$$

$$\frac{\partial e}{\partial t} = -\nabla \cdot (e \mathbf{u}) - P \nabla \cdot \mathbf{u} + Q_v + Q_J + Q_{\text{cool}}, \quad (3)$$

$$\frac{\partial \mathbf{B}}{\partial t} = \nabla \times (\mathbf{u} \times \mathbf{B}) + \frac{1}{\text{Re}_m} \nabla^2 \mathbf{B}, \quad (4)$$

where ρ is the fluid density, \mathbf{u} is the velocity, P the pressure, \mathbf{j} is the electric current density, \mathbf{B} is the magnetic field density and e is the internal energy. In Eq. (2) $\mathbf{j} \times \mathbf{B}$ is the Lorentz force giving rise to the Lorentz work W_L . Q_v and Q_J are the viscous and Joule dissipation respectively. Q_{cool} is a Newtonian cooling term and Re_m is the magnetic Reynolds number. \mathbf{f} is an external prescribed forcing term with an amplitude that is allowed to evolve with time, keeping the average kinetic energy approximately constant through both laminar and turbulent phases, cf. Archontis et al. (2003b).

Equations Eq. (1-4) are solved numerically on a staggered mesh using derivatives and interpolations that are of 6th and 5th order respectively in a numerical scheme that conserves $\nabla \cdot \mathbf{B} = 0$ exactly. Numerical solutions are obtained on a grid of 128^3 points, the code by Nordlund and others e.g. Nordlund et al. (1992).

The chosen initial velocity field is similar to the classical ABC flow (Dorch, 2000) but does not contain cosine terms:

$$\mathbf{u} = (\sin z, \sin x, \sin y), \quad (5)$$

where the coordinates (x, y, z) have a periodicity of 2π in all directions. The total kinetic helicity $\int_V \mathbf{u} \cdot \boldsymbol{\omega} \, dV$ (where $\boldsymbol{\omega} = \nabla \times \mathbf{u}$ is the vorticity) is identically zero for this flow that has previously been found to be a good candidate for fast dynamo action: The growth rate of the magnetic field is known to increase as a function of Re_m in the linear regime, at least until $\text{Re}_m = 800$ (Galloway & Proctor, 1992). The initial magnetic seed field is chosen to be weak and divergence-free with an amplitude of 10^{-5} in non-dimensional units.

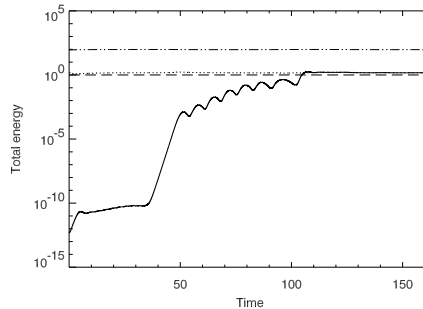


Figure 1. Total energies as a function of time for an experiment with $Re_m = 100$ and $Re = 2$. Here the solid curve is magnetic energy E_{mag} , the dotted curve kinetic energy E_{kin} and the dotted-dashed curve the total thermal energy E_{th} . The dashed horizontal line indicates unity energy.

3. Results and discussion

We have performed several numerical experiments with varying magnetic Reynolds number Re_m between 50–200 and kinetic fluid Reynolds number Re between 2–450.

Initially during the linear, kinematic regime the total magnetic energy E_{mag} grows exponentially because of a small difference between Lorentz work W_L and the Joule dissipation Q_J . Figure 1 shows the evolution of total energy in an experiment with $Re_m = 100$ and $Re = 2$: In this case the magnetic field was initially give by a weak *uniform* seed field and this special topology results in several linear dynamo modes being excited, but eventually E_{mag} saturates at equipartition within a few fractions of a percent.

The balance between W_L and Q_J in the linear regime does not hold in places with weak magnetic field and little dissipation, as has also been shown in previous kinematic dynamo experiments (Archontis et al., 2003a). A calculation, for low Re , of the average net work $-W_L - Q_J$ yields that most of the work responsible for the fast dynamo action, occurs in places with less than 20% of the maximum dissipation and magnetic field strength and occupies 98% of the volume. There, the net work is 95% of the maximum work level. In the remaining 2% of the volume the strong dissipation is balanced by the work done on the field by the flow through advection and convergence.

If the magnetic field is initialized by a *random* seed field fewer linear modes appear before saturation: Figure 2 (left) shows magnetic energy as a function of time for a case with $Re_m = 100$ and $Re = 50$ that also saturates near equipartition, but only has one dominant, very fast growing mode during the linear regime.

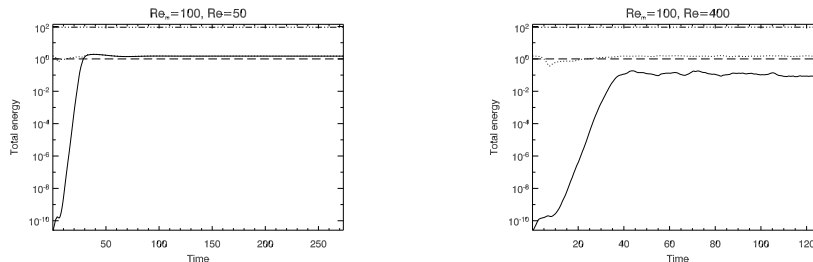


Figure 2. Total magnetic, kinetic and thermal energy as functions of time for cases with $Re_m = 100$ and $Re = 50$ (left) and $Re_m = 100$ and $Re = 400$ (right). Line styles are the same as in Fig. 1.

In these cases where Re is low, the flows are very laminar, as we shall show below, but if Re is increased turbulence sets in. With well-developed turbulence the magnetic energy saturates significantly below equipartition as can be seen in Fig. 2 (right) for a case also with $Re_m = 100$ but $Re = 400$, where in the non-linear regime $E_{\text{mag}} \approx 0.2 E_{\text{kin}}$. This dependence on Re is summarized in Fig. 3 (left) that shows the deviation from exact equipartition, after saturation, as a function of Re for three different values of Re_m : Apparently there is a jump at $Re \sim 300$ below which the dynamo saturates at exact equipartition. This scenario can also be quantified in terms of magnetic Prandtl number Pr_m . There is a critical value $Re^{(c)}$ below which the dynamo saturates below equipartition and the value of $Re^{(c)}$ depends on Pr_m roughly as $Re^{(c)} \sim 50 Pr_m^{0.5}$. At sufficiently low Pr_m the dominating dynamo mode is in fact a decaying mode, see e.g. Fig. 3 (right) that shows the behavior of the total energy for a case with $Re_m = 50$ and $Re = 300$ corresponding to $Pr_m = 1/6$.

A tell-tale result is that the flow (for low Re), after it goes through a turbulent phase just prior to saturation, comes out as a laminar solution with the magnetic and velocity field parallel and equal in magnitude, see Fig. 5 (left): E.g. for the experiment with $Re_m = 200$ and $Re = 200$ less than 2% of the volume is occupied by field and flows inclined by more than 10° . In this case, with unit magnetic Prandtl number Pr_m , the viscous and resistive losses are both directly proportional to the velocity and magnetic field strength, respectively, with the same constant of proportionality and equal to $1/Re$. For $Pr_m \neq 1$ the two fields are still proportional but not exactly equal and the saturation level deviates from exact equipartition in fractions of a percent.

In fact, there are marked differences between the structure of the magnetic and velocity fields in the experiments as Re is increased: This is true both in Fourier k -space as well as in physical space. In k -space,

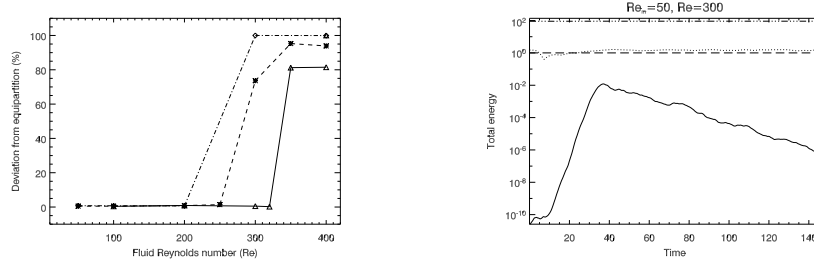


Figure 3. Left: A summary figure of the deviation (in percent) from saturation at exact equipartition as a function of fluid Reynolds number Re . Three regimes are shown corresponding to experiments with $Re_m = 200$ (full curve), $Re_m = 100$ (dashed curve) and $Re_m = 50$ (dashed-dotted curve). Right: Total magnetic, kinetic and thermal energy as functions of time for an experiment with $Re_m = 50$ and $Re = 300$ corresponding to $Pr_m = 1/6$ (right figure). Line styles are the same as in Fig. 1.

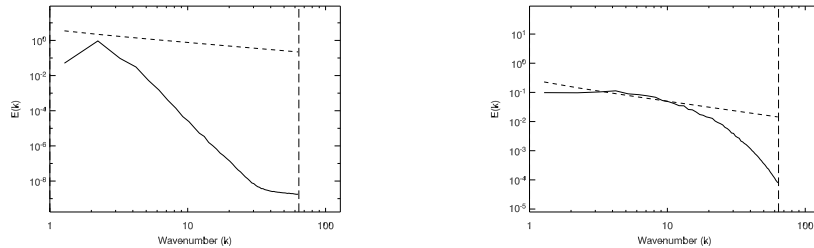


Figure 4. Energy spectra of magnetic energy as function of wavenumber k for for a case with $Re_m = 50$ and $Re = 200$ (left), and a case with $Re_m = 200$ and $Re = 450$ (right).

for $Re_m = 200$ and $Re = 200$, the magnetic and kinetic energy power are completely coincident (with a ratio of ~ 0.95) except at the smallest scales where there is slightly more power in the flow. The magnetic energy has a maximum at $k \approx 2.2$ and the spectra approximately follow a power-law with a power of -3 , but for $k \geq 10$ become very steep, see Fig. 4 (left). In cases with $Re_m = 200$ and higher Re there is also a lot of power at large scales, but the spectrum is much flatter and roughly follows Kolmogorov scaling for intermediate wavenumbers, see Fig. 4 (right). Examination of the magnetic energy per wavenumber $kE(k)$ reveals that most energy comes from scales $k \approx 10$ similar to what was found in models of non-helical turbulence by Haugen et al. (2003).

In physical space, the behavior of the magnetic field and the velocity flow can be quite revealing. Hereafter, we consider first the situation with $Re \leq 200$ and then a higher $Re = 400$ case. During the exponential amplification of the magnetic energy, the magnetic field has the form of

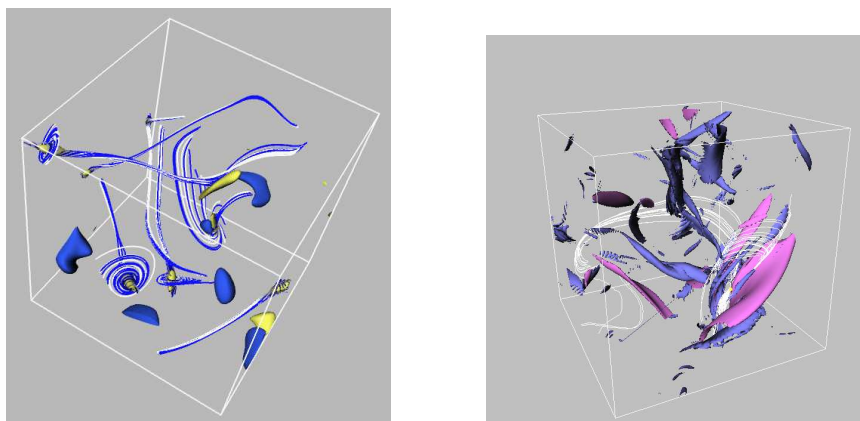


Figure 5. Left: Volume rendering of the magnetic field and velocity flow in the experiment with $Re_m = 200$ and $Re = 200$ during saturation. Isosurfaces of regions of low magnetic field and flow (light structures) and local maxima (dark). The lines are magnetic field lines (dark) and stream lines (light). Right: Strong magnetic field (light) and vorticity structures (dark) in the experiment $Re_m = 200$ and $Re = 400$ during saturation. Field lines traced from weak magnetic field (left side of the box) are stretched and pile up in twisted sheets around strong vortex tubes (to the right).

strong sheets or tubes which are spiraling around strong vortex tubes, cf. Fig. 5 (left). The weak background field is stretched by the flow and is folded against the sheets in a highly twisted manner. In the saturation regime the flow and the magnetic field have a less complex configuration and consist of regions with stagnation points. Figure 5 (left) illustrates that there are two kinds of flow stagnation points with spiraling streamlines in a plane perpendicular to an axis of convergence or divergence, respectively: Near the center of Fig. 5 (left) almost on a vertical line, it is illustrated how a stagnation point with a spiral plane connects to a second stagnation point where the field and stream lines form a plane perpendicular to an axis that in turn approaches the spiral plane of the first stagnation point. Magnetic null-points coincide with flow stagnation points, and sites of maximum magnetic flow and field strength coincide; here the magnetic and velocity fields take the form of collapsed “blobs” of parallel field and stream lines that have been folded and intensified. Next to these are sheets of strong vorticity.

In the case of the experiments with high Re that saturates below equipartition, there are fluctuations in magnetic energy and time-intervals where E_{mag} increases or decreases (Fig. 2, right). During the increase most of the work occurs again in between the strong magnetic structures where dissipation is low. The velocity has still a good grip on the weakest part of the field and increases the magnetic energy by stretching the field lines. The magnetic field has the form of intermittent

flux tubes or sheets that are twisted around regions of high vorticity (Fig. 5, right). The twisting of the magnetic field increases the tension of the magnetic field lines and thereby the magnetic energy. Twisted sheets with like polarity merge and those with opposite polarity reconnect, with the most rapid release of energy occurring when E_{mag} is maximum. The reconnected field lines go back and replace the weak field which was initially stretched by the flow. When the magnetic energy decreases the field lines start to untwist and magnetic structures are split into smaller pieces. This mode is reminiscent of the kinematic ABC-flow dynamo that also exhibits an undulatory behavior of E_{mag} as magnetic field lines are first experiencing increased tension boosting E_{mag} , subsequently leading to reconnection decreasing E_{mag} but replenishing the supply of weak field for the flow to do Lorentz work on (Dorch, 2000). In this non-linear case however, there is no periodic behavior and there is no symmetry to the flow, in the form of e.g. stagnation points and hence the reconnected weak magnetic field lines are not twisted to form new flux tubes by the same velocity structures that formed their “ancestors”.

4. Conclusion

We have presented results from new numerical experiments with non-linear dynamo action by a non-helical flow while varying characteristic dimensionless parameters: No matter whether in the linear or saturated regimes, or whether the flow is laminar or turbulent, dynamo action occurs primarily where the field is weak. 3-d visualization of the flow and the magnetic field shows similar structures associated with stretching, folding and subsequent amplification of the magnetic energy, in both the linear and non-linear equilibrated regime. Additionally, we find that there is a critical fluid Reynolds number above which the dynamo no longer saturates at or close to equipartition, but at a lower level characteristic of turbulent astrophysical dynamos. In terms of energy spectra there are marked differences between the high and low Re cases, but in physical space we identify some individual common processes that are likely to be a major part of the dynamo mechanism. Our intention was to illustrate that studying dynamo action by these kind of flows is a viable way to understand astrophysical dynamos. In a forthcoming paper we will follow up with a broad analysis in physical space of the numerical experiments presented here: We believe that the key to understanding the nature of non-linear dynamo action is to answer such questions as “where do the magnetic field lines come from, and where do they go?”

Acknowledgements

SBFD was supported by the Danish Natural Science Research Council. Access to computational resources granted by the Danish Center for Scientific Computing is acknowledged.

References

- Archontis, V., Dorch, S.B.F. and Nordlund, Å.: 2003a, *Astron. Astrophys.* **397**, 393.
Archontis, V., Dorch, S.B.F. and Nordlund, Å.: 2003b, *Astron. Astrophys.* **410**, 759.
Cattaneo, F., Hughes, D.W., and Kim, E.: 1996, *Phys. Rev. Letters* **76**, 2057.
Childress, S. and Gilbert, A.D.: 1995, *Stretch, Twist, Fold: The Fast Dynamo*, Springer-Verlag, Berlin, p.52.
Choudhuri, A.R.: 2003, *Solar Phys.* **215**, 31.
Dorch, S.B.F.: 2000, *Physica Scripta* **61**, 717
Galloway, D. and Proctor, M.: 1992, *Nature* **356**, 691.
Haugen, N.E.L., Brandenburg, A., and Dobler, W.: 2003, *Astrophys. J.* **597**, L141.
Moreno-Insertis, F., Caligari, P. and Schüssler, M.: 1994, *Solar Phys.* **153**, 449.
Nordlund, A., Brandenburg, A., Jennings, R.L., Rieutord, M., Roukolainen, J., Stein, R.F., and Tuominen, I.: 1992, *Astrophys. J.* **392**, 647.
Parker, E.N.: 1979, *Cosmical Magnetic Fields*, Clarendon, Oxford.
Safier, P.N.: 1999, *Astrophys. J.* **510**, L127.
Tanner, S. and Hughes, D.: 2003, *Astrophys. J.* **586**, 585.

